Electronic Supporting Information

Optimized Trimetallic Benzotriazole-5-carboxylate MOFs with Coordinately Unsaturated Active site as Efficient Electrocatalyst for Oxygen Evolution Reaction

Jian-Tao Yuan, Juan-Juan Hou*, Xue-Li Liu, Ya-Ru Feng, and Xian-Ming Zhang*

Key Laboratory of Magnetic Molecules & Magnetic Information Materials Ministry of Education, School of Chemical and Material Science, Shanxi Normal University, Linfen, 041004, China

Figure S1. a) View of the $Co_3(OH)_2$ chain; b) The coordination environments of the cobalt ion; and c) The 3D framework of **Co_3-btca** with 1D channels.

Figure S2. a) Powdered X-ray diffraction (PXRD) patterns of **$Co_{3-x}Fe_x$-btca**; b) PXRD patterns of **$Co_{3-x}Fe_x$-btca** in 1M KOH for 8 h.

Figure S3. a) Powdered X-ray diffraction (PXRD) patterns of **$Co_{3-x-y}Fe_xNi_y$-btca**; b) PXRD patterns of **$Co_{3-x-y}Fe_xNi_y$-btca** in 1M KOH for 8 h.

Figure S4. IR spectra of **M-btca.**

Figure S5. TG analysis of **M-btca**.

Figure S6. XPS survey spectra of a) **Co-btca**; b) **$Co_{2.79}Fe_{0.21}$-btca**; c) **$Co_{2.36}Fe_{0.19}Ni_{0.45}$-btca**.

Figure S7. CV curve between 0.892–0.992 vs. RHE for a) **Co-btca**; b) **$Co_{2.74}Fe_{0.26}$-btca**; c) **$Co_{2.77}Fe_{0.23}$-btca;** and d) **$Co_{2.79}Fe_{0.21}$-btca**.

Figure S8. CV curve between 0.892–0.992 vs. RHE for a) **$Co_{1.25}Fe_{0.83}Ni_{0.92}$-btca**; b) **$Co_{2.36}Fe_{0.19}Ni_{0.45}$-btca**.

Figure S9. The electrochemical impedance spectroscopy (EIS) of **M-btca** in 1 M KOH.

Figure S10. The equivalent model for fitting electrochemical impedance data of OER (**$Co_{2.36}Fe_{0.19}Ni_{2.45}$-btca**).

Figure S11. Chronopotentiometric curves of **Co-btca**, **$Co_{3-x}Fe_x$-btca** and **$Co_{1.23}Fe_{0.83}Ni_{0.92}$-btca** at its overpotential corresponding to the current density of 10 mA cm^{-2}.

Figure S12. XRD patterns of **$Co_{2.36}Fe_{0.19}Ni_{0.45}$-btca** on GCE ($\phi$ = 3 mm) after the first 33 h, and 74 h with a scan rate of 5 mV s^{-1}.

Figure S13. High resolution XPS spectra of Co2p in **$Co_{2.36}Fe_{0.19}Ni_{0.45}$-btca** after the first 33 h, and 74 h.

Figure S14. High resolution XPS spectra of Ni2p in **$Co_{2.36}Fe_{0.19}Ni_{0.45}$-btca** after the first 33 h, and 74 h.

Figure S15. High resolution XPS spectra of Fe2p in **$Co_{2.36}Fe_{0.19}Ni_{0.45}$-btca** after the first 33 h, and 74 h.

Table S1. Crystal data and structure refinement for **M-btca**.

Table S2. Bond lengths [Å] for **M-btca**.

Table S3. ICP analysis for **M-btca**.

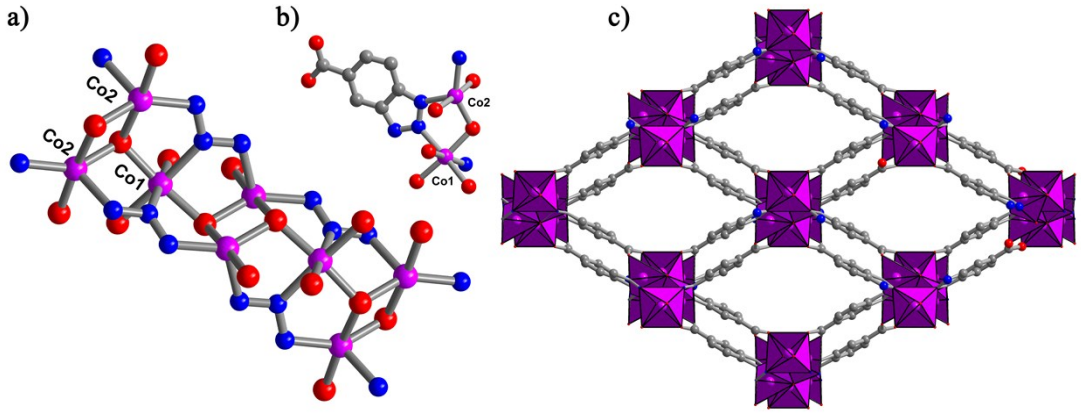

Figure S1. a). The 1D $Co_3(OH)_2$ chain in **Co_3-btca**; b). The coordination environments of the cobalt ion; c). The 3D framework of **Co_3-btca** with 1D channel.

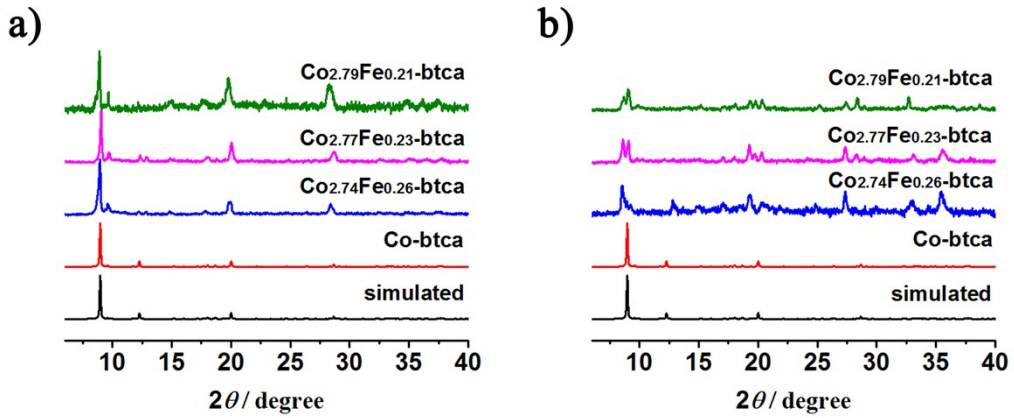

Figure S2. a).Powdered X-ray diffraction (PXRD) patterns of **$Co_{3-x}Fe_x$-btca**; b). PXRD patterns of **$Co_{3-x}Fe_x$-btca** in 1M KOH for 8 h.

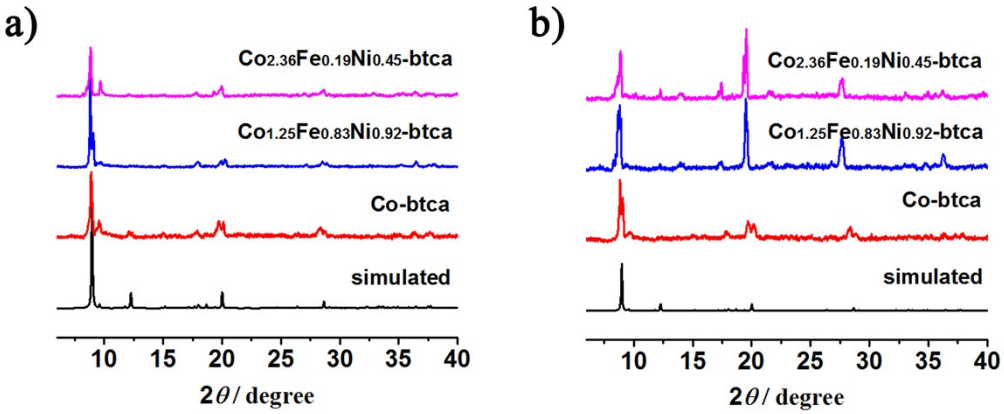

Figure S3. a) Powdered X-ray diffraction (PXRD) patterns of **$Co_{3-x-y}Fe_xNi_y$-btca**; b) PXRD patterns of **$Co_{3-x-y}Fe_xNi_y$-btca** in 1M KOH for 8 h.

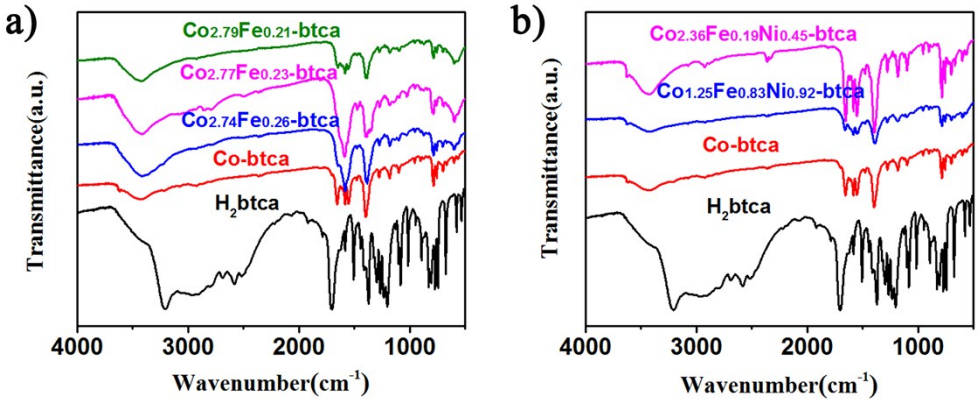

Figure S4. IR spectra of **M-btca**.

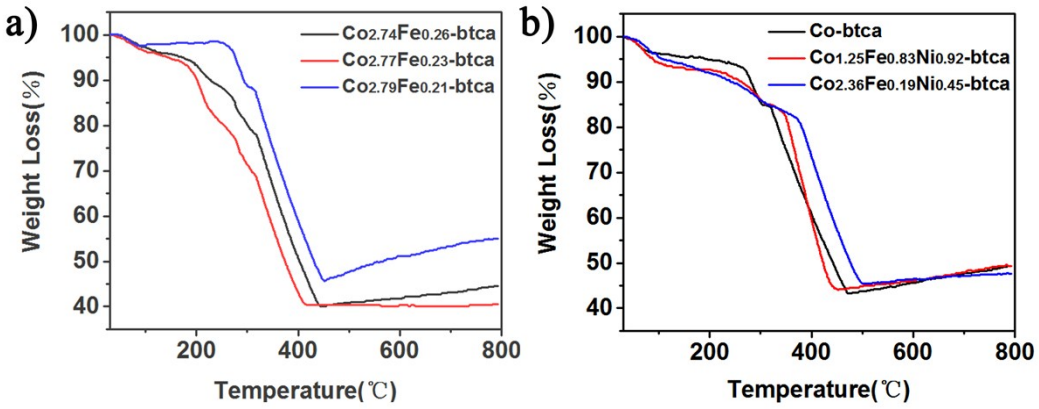

Figure S5. TG analysis of **M-btca**.

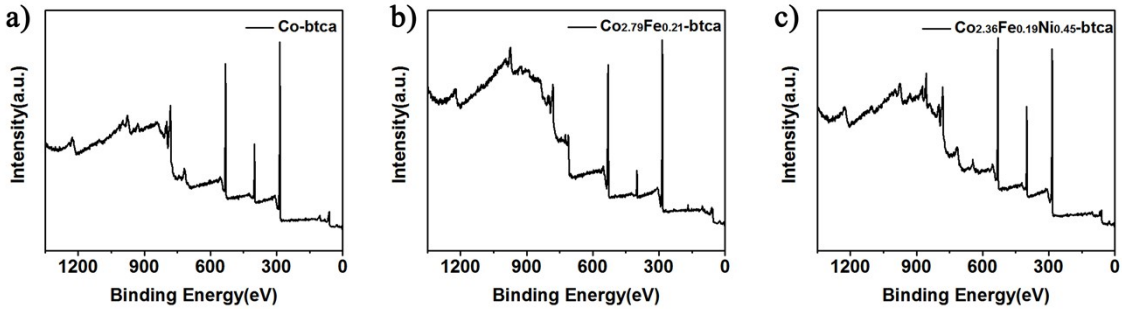

Figure S6. XPS survey spectra of (a) **Co-btca**, (b) **$Co_{2.79}Fe_{0.21}$-btca**, (c) **$Co_{2.36}Fe_{0.19}Ni_{0.45}$-btca**.

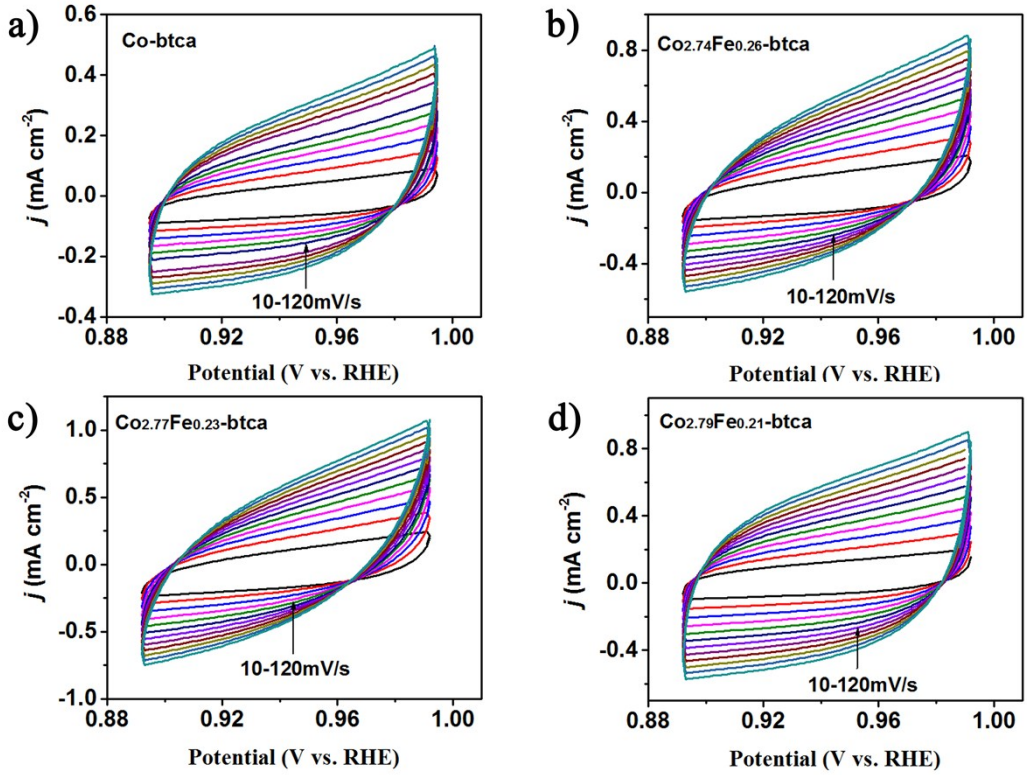

Figure S7. CV curve between 0.892–0.992 vs. RHE for a) **Co-btca**; b) **$Co_{2.74}Fe_{0.26}$-btca**; c) **$Co_{2.77}Fe_{0.23}$-btca** and d) **$Co_{2.79}Fe_{0.21}$-btca**.

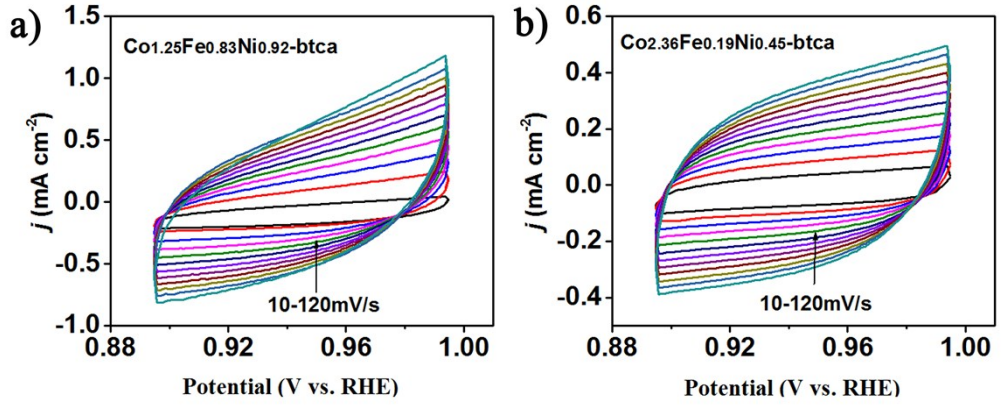

Figure S8. CV curve between 0.892–0.992 vs. RHE for a) **$Co_{1.25}Fe_{0.83}Ni_{0.92}$-btca**; b) **$Co_{2.36}Fe_{0.19}Ni_{0.45}$-btca**.

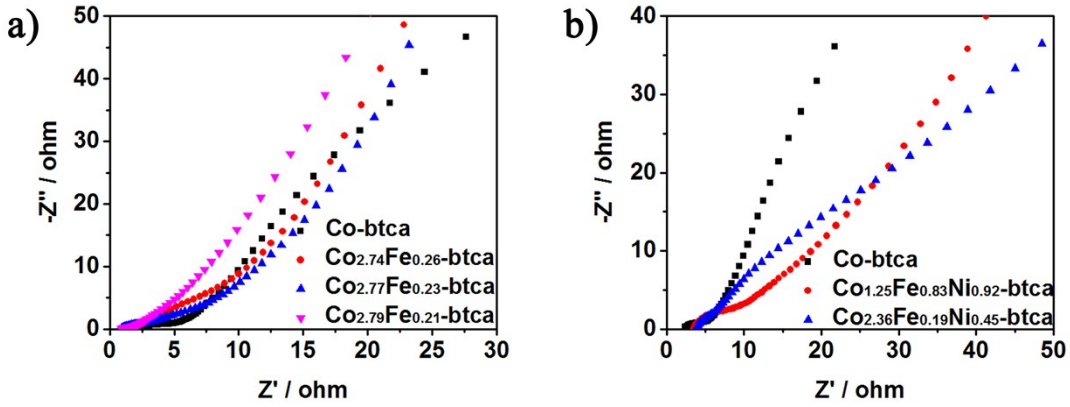

Figure S9. The electrochemical impedance spectroscopy (EIS) of **M-btca** in 1 M KOH.

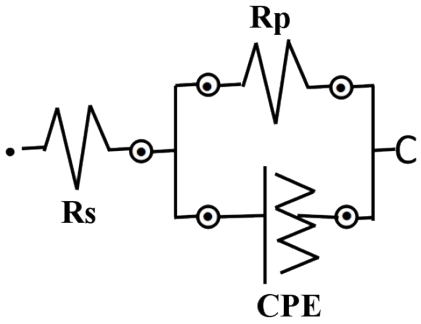

Figure S10. Equivalent circuit model for fitting electrochemical impedance data of OER (**$Co_{2.36}Fe_{0.19}Ni_{2.45}$-btca**).

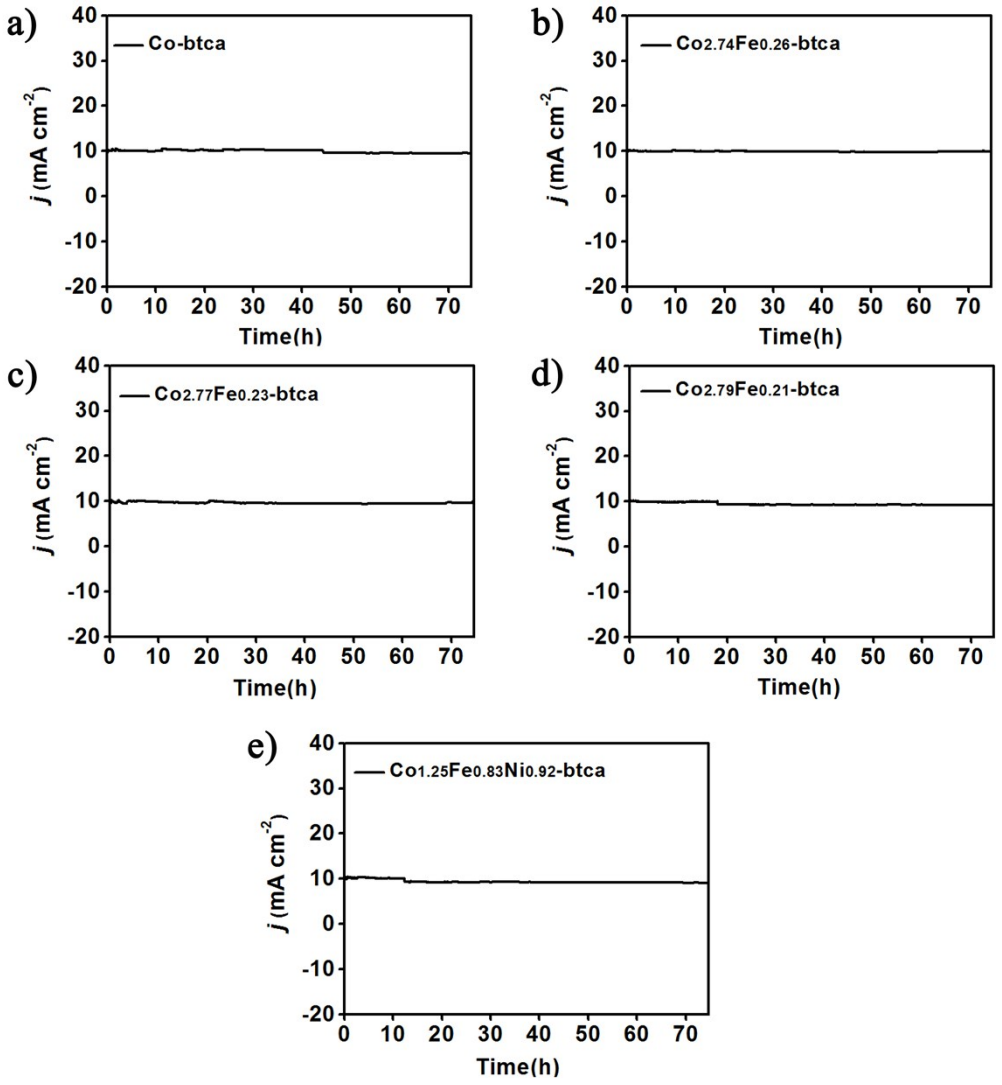

Figure S11. Chronopotentiometric curves of **Co-btca**, **$Co_{3-x}Fe_x$-btca** and **$Co_{1.23}Fe_{0.83}Ni_{0.92}$-btca** at its overpotential corresponding and 10 mA cm^{-2}.

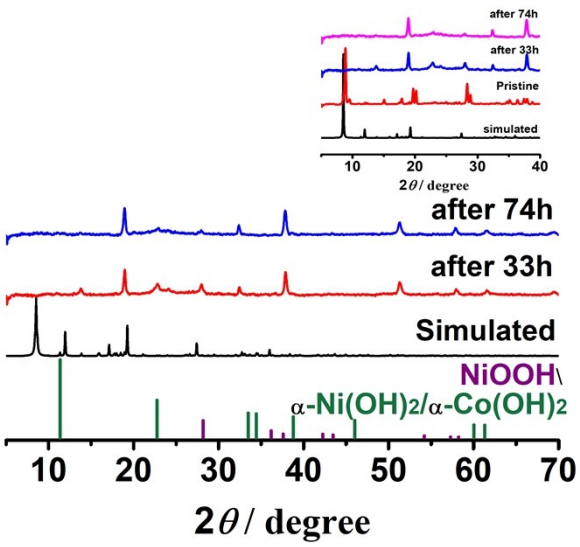

Figure S12. XRD patterns of **$Co_{2.36}Fe_{0.19}Ni_{0.45}$-btca** on GCE ($\phi$ = 3 mm) after the first 33 h, and 74 h with a scan rate of 5 mV s^{-1}.

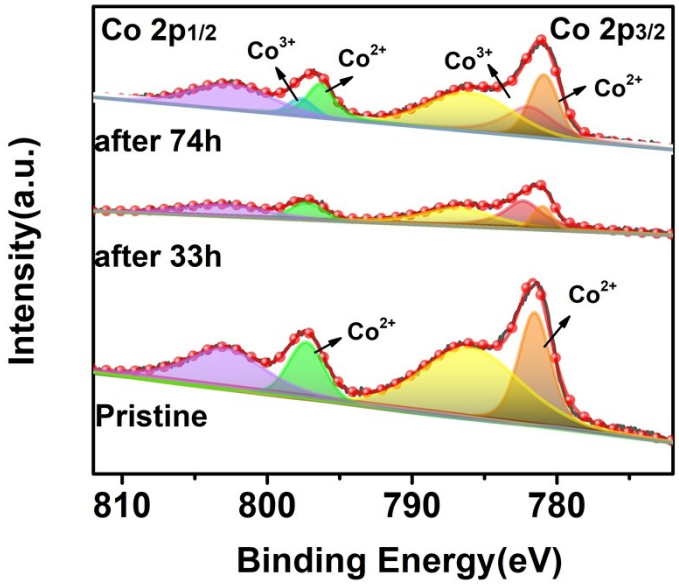

Figure S13. High resolution XPS spectra of Co2p in **$Co_{2.36}Fe_{0.19}Ni_{0.45}$-btca** after the first 33 h, and 74 h.

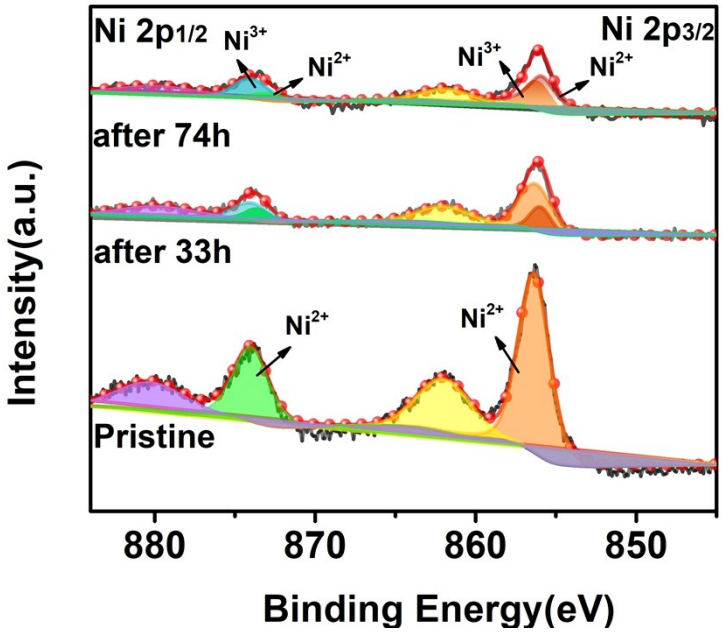

Figure S14. High resolution XPS spectra of Ni2p in **$Co_{2.36}Fe_{0.19}Ni_{0.45}$-btca** after the first 33 h, and 74 h.

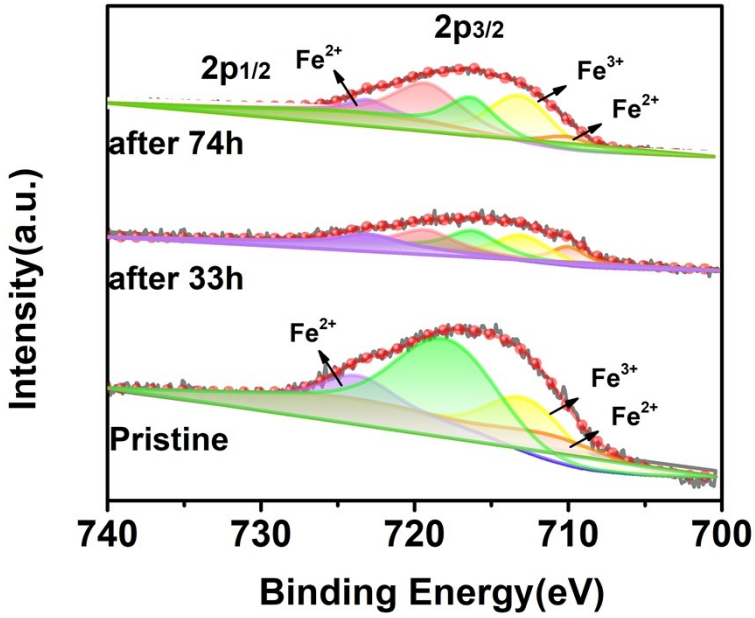

Figure S15. High resolution XPS spectra of Fe2p in **$Co_{2.36}Fe_{0.19}Ni_{0.45}$-btca** after the first 33 h, and 74 h.

Table S1. Summary of Crystal data and structure refinement Parameters for **M-btca.**

Empirical formula	$C_{14}H_7Co_3N_6O_6$	$C_{14}H_7Co_{2.79}Fe_{0.21}N_6O_6$	$C_{14}H_7Co_{2.36}Fe_{0.19}Ni_{0.45}N_6O_6$
Fw	532.05	531.40	530.38
Tem./K	293(2)	293(2)	293(2)
Crys.Sys.	Monoclinic	Monoclinic	Monoclinic
SpaceG.	C2/c	C2/c	C2/c
a / Å	18.453(2)	17.648(6)	17.7685(9)
b / Å	11.663(2)	13.038(4)	12.7627(9)
c / Å	11.0742(10)	11.183(2)	11.2090(5)
α /°	90	90	90
β / °	94.348(9)	95.34(3)	95.114(4)
γ / °	90	90	90
V / Å^3	2376.4(6)	2562.1(13)	2531.8(2)
Z	4	4	4
ρ_{calc} / mg/mm^3	1.487	1.378	1.391
μ / m/mm^{-1}	2.105	1.936	2.908
F(000)	1048	1047	1056
2θ/°	3.494-26.994	3.622-26.990	4.271-73.043
Data/restr/para	2563/0/132	2746/0/132	2523/0/132
S	1.020	1.004	1.051
R_1,[a] wR_2 [b] [I>2σ (I)]	0.0691, 0.1395	0.0591, 0.1126	0.0651, 0.1747
R_1,[a] wR_2 [b] [all data]	0.1185, 0.1713	0.1093, 0.1338	0.0893, 0.1888

$\Delta\rho_{max}/\Delta\rho_{min}$ / e Å^{-3}	0.972/-0.719	0.687 / -0.643	0.725 / -0.765

[a] $R_1 = \sum||F_o|-|F_c||/\sum|F_o|$, b. $wR_2 = [\sum w(F_o^2-F_c^2)^2/\sum w(F_o^2)^2]^{1/2}$

Table S2. Bond lengths [Å] for **M-btca**

	$C_{14}H_7Co_3N_6O_6$	$C_{14}H_7Co_{2.79}Fe_{0.21}N_6O_6$	$C_{14}H_7Co_{2.36}Fe_{0.19}Ni_{0.45}N_6O_6$
M(1)-O(4a)	2.029(4)	2.062(3)	2.055(3)
M(1)-O(4)	2.030(4)	2.062(3)	2.055(3)
M(1)-O(2a)	2.110(5)	2.074(4)	2.085(3)
M(1)-O(2)	2.110(5)	2.074(4)	2.085(3)
M(1)-N(2b)	2.150(5)	2.131(5)	2.133(4)
M(1)-N(2c)	2.150(5)	2.131(5)	2.133(4)
M(2)-O(4)	2.019(4)	2.013(4)	2.005(3)
M(2)-O(1)	2.054(5)	2.037(4)	2.036(4)
M(2)-N(1d)	2.084(5)	2.072(5)	2.075(4)
M(2)-N(3b)	2.123(5)	2.079(4)	2.079(4)
M(2)-O(4e)	2.176(5)	2.171(4)	2.154(3)

Symmetry transformations used to generate equivalent atoms: a) -x+1, -y+2, -z+2; b) -x+2, -y+2, -z+2; c) x-1, y, z; d) -x+1, -y+1, -z+2; e) -x, -y, -z+1; f) x+1, y, z.

Table S3. ICP analysis for **M-btca**.

	$Co_{2.74}Fe_{0.26}$-btca	$Co_{2.77}Fe_{0.23}$-btca	$Co_{2.79}Fe_{0.21}$-btca
Wt%	Co:17	Co:17.47	Co:18.41
	Fe:1.52	Fe:1.24	Fe:1.43
Co/Fe	0.26:2.74	0.23:2.77	0.21:2.79
	$Co_{1.25}Fe_{0.83}Ni_{0.92}$-btca	$Co_{2.36}Fe_{0.19}Ni_{0.45}$-btca	
	Co:17.81	Co:19.04	
Wt%	Fe:11.32	Fe:1.47	
	Ni:12.01	Ni:3.64	
Co/Fe/Ni	0.83:1.25:0.92	0.19:2.36:0.45	